Biochemistry

 Volume 32, Number 21 June 1, 1993

Accelerated Publications

Thermodynamic Characterization of the Structural Stability of the Coiled-Coil Region of the bZIP Transcription Factor GCN4†

Kelly S. Thompson,‡ Charles R. Vinson,§ and Ernesto Freire*,‡

Department of Biology and Biocalorimetry Center, The Johns Hopkins University, Baltimore, Maryland 21218, and Laboratory of Biochemistry, National Cancer Institute, National Institutes of Health, Bethesda, Maryland 20892

Received February 26, 1993; Revised Manuscript Received April 6, 1993

ABSTRACT: The thermal stability of a 56 amino acid fragment of GCN4 has been studied by high-sensitivity differential scanning calorimetry and circular dichroism spectroscopy. This fragment contains the leucine zipper and part of the basic region. The thermal unfolding of GCN4–56 is a reversible process and can be well represented by a reaction of the form $N_2 \leftrightarrow 2U$, indicating that the unfolding of the leuzine zipper is a two-state process in which the helices are only stable when they are in the coiled-coil conformation. As expected, the transition temperature is concentration dependent. At pH 7.06 and a protein concentration of 5×10^{-4} M the transition temperature is close to 70 °C while at 5×10^{-6} M it is close to 50 °C. The enthalpy change for unfolding is 31.5 kcal mol^{-1} at 70 °C. Since the isolated helices are unstable, interactions at the interface between the two helices play a key role in the stabilization of the native dimer. These interactions primarily involve the burial of apolar surface from the solvent (hydrophobic effect) and electrostatic interactions. Structural thermodynamic calculations have permitted a dissection of the magnitude of the various contributions to the total Gibbs free energy of stabilization.

Landshultz et al. (1988) first proposed the leucine zipper model for the dimerization region of C/EBP, GCN4, and the Fos/Jun heterodimer. Since that time there has been intense interest in the characterization of the dimerization and DNA binding interactions of this class of proteins largely because of their role in transcriptional regulation and, in some cases, oncogenesis (Johnson & McKnight, 1989). Dimerization occurs through the formation of an α-helical coiled coil of 30–40 amino acids per strand, called the leucine zipper. This region is highly conserved and defined by a heptad repeated, $(abcdefg)_n$, in which the generally hydrophobic residues at positions a and d are on the same face of each of the helices in apposition to each other in the coiled coil (O'Shea et al., 1989, 1991; Gentz et al., 1989; Oas et al., 1990; Rasmussen et al., 1991). Immeditely N-terminal to the leucine zipper is a region rich in basic residues. Various mutagenesis (Gentz et al., 1989; Landshultz et al., 1989; Turner & Tjian, 1989) and subunit exchange (Agre et al., 1989) studies indicate that this basic region constitutes the DNA binding site and that the leucine zipper is required for its interaction with DNA.

The scissors grip model for the interaction of leucine zipper proteins with their DNA sequences proposes that, in the presence of DNA, the basic regions form extensions of the leucine zipper helices and that residues on one face of the basic region helix form a sequence-specific binding site for DNA (Vinson et al., 1989; O'Neil et al., 1990). Binding studies performed on a 58-residue GCN4 peptide show a striking increase in the α-helical content of the peptide upon interaction with DNA (Weiss, 1990; Weiss et al., 1990). In the absence of DNA, the basic region of GCN4, alone or in tandem with the leucine zipper region, is not highly structured and appears to form a highly flexible and loosely folded helix (Saudek et al., 1991).

† Supported by grants from the National Institutes of Health (RR04328) and the National Science Foundation (MCB-9118687).

* To whom correspondence should be addressed.

‡ The Johns Hopkins University.

§ National Cancer Institute, NIH.

0006-2960/93/0432-5491$04.00/0

While the structure of coiled coils in general, and leucine zippers in particular, has been extensively studied, the thermodynamic basis of their stability and folding mechanism is still not well understood. In this paper we have used the techniques of high-sensitivity differential scanning calorimetry (DSC) and circular dichroism (CD) spectroscopy to measure the thermodynamic parameters ΔH, ΔC_p, and ΔS that define the stability of a peptide containing the leucine zipper and part of the basic region of GCN4. The results of these studies indicate that the folding/unfolding of the peptide involves only two states, the native dimer and the unfolded monomer, with no significant population of folded monomers present. In addition, since the crystallographic structure of the GCN4 leucine zipper is available (O'Shea et al., 1991), we have been able to perform a structural thermodynamic analysis of GCN4. These studies suggest that the part of the basic region included in GCN4–56 contributes little to the stability of the leucine zipper.

MATERIALS AND METHODS

Materials. Sodium phosphate, KCl, and EDTA were obtained from J. T. Baker Inc. Spectra/por 3 dialysis membrane was purchased from Spectrum.

Protein Purification and Determination of Concentration. The 56 amino acid GCN4 peptide fragment was purified as described previously for C/EBP62 (Shuman et al., 1990). The sequence of the peptide is NH_2-GSAALKRARN-TEAARRSRARKLQRMKQLEDKVEELLSKNYHLE-NEVARLKKLVGER-COOH. The sequence spans from residue 228 to the C-terminus of the wild-type protein, with Gly-Ser appended to the N-terminus of the peptide. Samples were dialyzed overnight at 4 °C against 4 L of 12.5 mM potassium phosphate, 25 mM KCl, and 0.25 mM EDTA, pH 7.06, through Spectra/por 3 dialysis membrane. The peptide concentration was determined spectrophotometrically using an extinction coefficient of $\epsilon_{274.5} = 1.605 \times 10^3\ M^{-1}\ cm^{-1}$ (Jon Shuman, personal communication).

Differential Scanning Calorimetry (DSC). Samples containing 1.02–3.3 mg mL^{-1} peptide were scanned at 60 °C h^{-1} in a DASM-4M microcalorimeter under 5.4 kg cm^{-1} pressure. The calorimeter was interfaced to a PC microcomputer equipped with a Data Translation DT-2801 A/D converter board for instrument control and automatic data collection. The excess heat capacity function was analyzed after scan rate normalization, concentration normalization, and baseline subtraction as described before using software developed in this laboratory (Xie et al., 1991).

Circular Dichroism Spectroscopy (CD). All CD experiments were performed using a Jasco J-710 spectropolarimeter interfaced to a PC microcomputer for automatic data collection. Wavelength scans were performed at discrete temperatures from 24 to 68 °C at a peptide concentration of 10 μM in a 5-mm rectangular CD cell. For each temperature point, spectra were obtained by averaging five wavelength scans collected at 1-nm intervals from 190 to 240 nm at a rate of 5 nm min^{-1}, a response time of 8 s for each point, and a bandwidth of 1 nm. Wavelength scans were processed by subtracting buffer scans taken at the same temperatures and normalizing for concentration to obtain the mean residue ellipticity. Temperature was maintained using a Haake F3 circulating water bath connected to a water-jacketed cell holder. Temperature was monitored using a Micro-therm 1006 thermometer and an S/N 117.C temperature probe (both from Hart Scientific) in physical contact with the peptide solution.

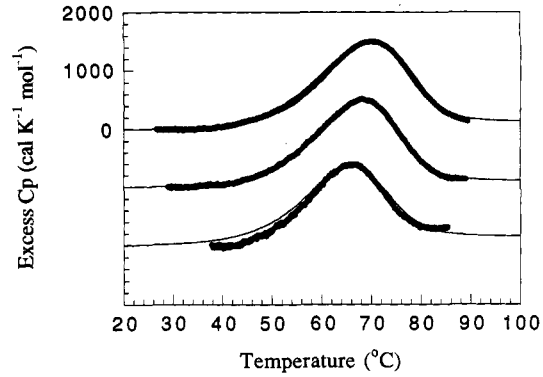

FIGURE 1: Excess heat capacity of GCN4 as a function of concentration. The concentrations are, from top to bottom, 504, 334.5, and 156 μM. Experiments were performed at pH 7.06 in 12.5 mM potassium phosphate, 25 mM KCl, and 0.25 mM EDTA. Experimental data are represented by filled circles. Theoretical curves generated with the parameters shown in Table I are represented by solid lines. For ease of presentation the data sets have been offset by 1 kcal (K·mol)$^{-1}$ below the 504 μM data set.

Temperature scans were performed on samples from 1 to 20 μM by scanning continuously from 10 to 80 °C. Data were collected using the time scan mode of the Jasco J-710 software. The ellipticity at 222 nm was recorded every 20 s with a response time of 0.5 s and a bandwidth of 1 nm. Θ_{222} and temperature were manually recorded at discrete points at an interval of about 5 °C, and intermediate temperatures were interpolated for every intervening ellipticity reading to yield a complete description of Θ_{222} vs temperature. Ellipticity readings were normalized to fraction unfolded using the standard equation

$$P_U = (\Theta - \Theta_N)/(\Theta_D - \Theta_N)$$

where Θ_N and Θ_D represent the ellipticity values for the fully folded and fully unfolded species at each temperature as calculated from the linear regression of the baselines preceding and following the transition region. Temperature was controlled using a Haake PG 20 temperature programmer interfaced to the Haake F3 circulating water bath and was continuously increased at a rate of 60 °C h^{-1}.

RESULTS AND DISCUSSION

Calorimetric and CD Experiments. A family of high-sensitivity calorimetric scans of GCN4–56 obtained at pH 7.06 (12.5 mM potassium phosphate, 25 mM KCl, 0.25 mM EDTA) and at protein concentrations ranging between 150 and 500 μM is shown in Figure 1. Lower concentrations could not be measured by calorimetry due to instrument sensitivity. At the highest concentration studied the transition is characterized by the presence of a peak located at 70 °C, an enthalpy change (ΔH) of 31.5 kcal mol^{-1}, and a heat capacity difference between the unfolded and native states (ΔC_p) of 135 ± 150 cal (K·mol)$^{-1}$ (all thermodynamic parameters in this paper are expressed on a *per mole of monomer* basis unless otherwise noted; also, following the standard convention, all thermodynamic parameters are referenced to the native state). As illustrated in the figure, the transition temperature decreases as the protein concentration decreases (see also Figure 5), consistent with the idea that the unfolding transition is coupled to the dissociation of the two subunits of GCN4. This effect is also reflected by the asymmetry of the heat capacity function, which in each case is skewed toward the low-temperature side of the transition (Freire, 1989). Under all conditions studied the transitions were reversible, as demonstrated by the recovery of the original signal in repeated scans of the same sample.

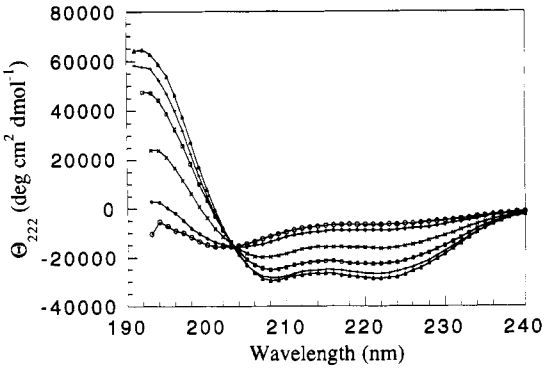

FIGURE 2: Far-UV CD spectra of 10 μM GCN4 as a function of temperature. The temperatures are, from highly structured to random coil, 24, 33, 41, 50, 59, and 68 °C. Experiments were performed at pH 7.06 in 12.5 mM potassium phosphate, 25 mM KCl, and 0.25 mM EDTA.

The nature of the thermal unfolding transition was also studied by circular dichroism (CD) spectroscopy. For these experiments the CD spectra in the 190–240-nm wavelength range was measured as a function of temperature and GCN4 concentration. Figure 2 shows the family of temperature curves obtained at 10 μM. An important conclusion from these data is that, at all temperatures, the measured spectra are well represented by the population-weighted superposition of the characteristic spectra for α-helix and random coil conformations. This is further substantiated by the presence of a well-defined isodichroic point at 203.4 nm, as expected for a system in which only two conformations are present. The content of α-helix is maximal at temperatures below the transition and decreases to zero at temperatures above the transition region.

Statistical Thermodynamic Analysis. In order to assess whether the folding/unfolding transition of GCN4–56 involves only two states (folded dimers and unfolded monomers) or includes the presence of a significant population of intermediates (folded monomers), the data were analyzed in terms of the complete statistical thermodynamic equations for the three-state system. Figure 3 graphically illustrates the basic definitions required for the statistical thermodynamic analysis of that system. According to the definitions, the population of molecules in the native (P_{N_2}), intermediate (P_I), and unfolded (P_U) states can be written as

$$P_{N_2} = 1/\{1 + K_1(4[N_2])^{-1/2} + K_2(4[N_2])^{-1/2}\} \quad (1a)$$

$$P_I = K_1(4[N_2])^{-1/2}/\{1 + K_1(4[N_2])^{-1/2} + K_2(4[N_2])^{-1/2}\} \quad (1b)$$

$$P_U = K_2(4[N_2])^{-1/2}/\{1 + K_1(4[N_2])^{-12} + K_2(4[N_2])^{-1/2}\} \quad (1c)$$

The statistical weights $K_1 = \exp(-\Delta G_1°/RT)$ and $K_2 = \exp(-\Delta G_2°/RT)$ are defined in the standard thermodynamic way in terms of the enthalpy, entropy, and heat capacity differences of those states relative to the native state. For each state i

$$\Delta G_i° = \Delta H_i°(T_i°) + \Delta C_{p,i}(T - T_i°) - T[\Delta S_i°(T_i°) + \Delta C_{p,i} \ln (T/T_i°)] \quad (2)$$

where $T_i°$ is the reference temperature. By definition, $\Delta G_i° = 0$ at this temperature. It must be noted that for a folding/unfolding transition coupled to a dissociation process this temperature does not coincide with the transition temperature (T_m) defined as the location of the peak maximum in the heat capacity function nor does T_m coincide with the temperature at which the transition is half-completed (Freire, 1989).

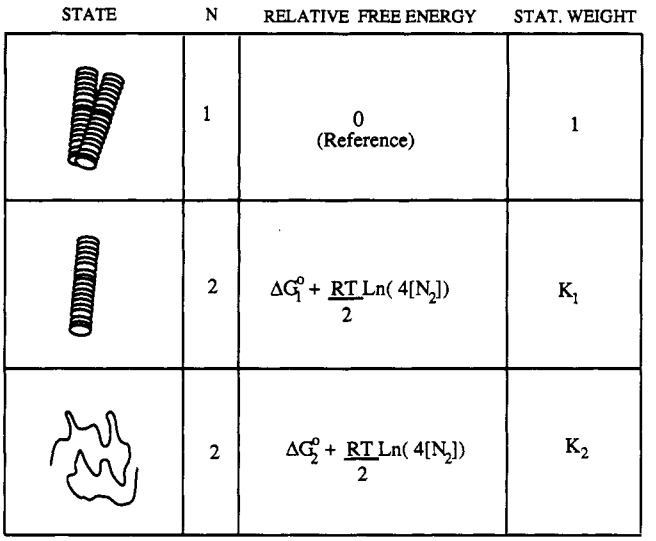

FIGURE 3: Schematic representation of the states, degeneracies, free energies, and statistical weights associated with the folding/unfolding equilibrium of the GCN4 leucine zipper. The states represented are the folded dimer, the folded monomer, and the unfolded monomer. $\Delta G_1°$ and $\Delta G_2°$ are the Gibbs free energies associated with the intermediate and unfolded states, and K_1 and K_2 are the stability constants defined in the standard way by $K_i = \exp(-\Delta G_i°/RT)$. $[N_2]$ is the concentration of folded dimers.

The total concentration of protein ($[P_T]$), expressed on a per monomer basis, is equal to

$$[P_T] = 2[N_2]\{1 + K_1(4[N_2])^{-1/2} + K_2(4[N_2])^{-1/2}\} \quad (3)$$

The population equations depend on the concentration of the native state (N_2) which is not known. Fortunately, $[N_2]$ can be written in terms of the known total concentration of protein ($[P_T]$) after solving eq 3:

$$[N_2] = \{A - (A^2 - 16[P_T]^2)^{1/2}\}/8 \quad (4)$$

where

$$A = 4[P_T] + (K_1 + K_2)^2$$

In order to analyze the calorimetric data, an expression for the average excess enthalpy function ($\langle \Delta H \rangle$) is needed (Freire & Biltonen, 1978). At any temperature, $\langle \Delta H \rangle$ for the system described in Figure 3 is equal to

$$\langle \Delta H \rangle = P_I \Delta H_I(T) + P_U \Delta H_U(T) \quad (5)$$

The excess heat capacity function ($\langle \Delta C_p \rangle$) measured by differential scanning calorimetry and shown in Figure 1 is simply the temperature derivative of eq 5. The analysis of the excess heat capacity function for GCN4 was performed in terms of the temperature derivative of eq 5 ($\langle \Delta C_p \rangle = \partial \langle \Delta H \rangle / \partial T$).

The experimental excess heat capacity data were analyzed in terms of the above formalism using a nonlinear least squares procedure as described elsewhere (Ramsay & Freire, 1990). It was found that, in all cases studied, the population of the intermediate state (P_I) was insignificant and did not contribute in any measurable way to the observed calorimetric signal. The thermal folding/unfolding transition was well represented by a two-state mechanism in which the only states significantly populated at all temperatures were native dimer and unfolded monomer. The solid lines in Figure 1 correspond to the theoretical curves with the best fit parameters to the exper-

Table I: Fitted Thermodynamic Parameters Associated with the Unfolding of GCN4–56 at Different Concentrations

	[GCN4–5] (μM)	T_m (°C)	$T°$ [a] (°C)	$\Delta H(T°)$ (kcal mol^{-1})	$\Delta S(T°)$ [cal (K·mol)$^{-1}$]	ΔC_p [b] [cal (K·mol)$^{-1}$]	SSR [c]
CD	1	41.4	93.9	33.9	92.4		0.14
	2	47.8	94.0	36.6	99.7		0.04
	5	51.2	94.3	35.9	97.7		0.02
	10	53.5	94.4	34.5	93.9		0.01
	20	54.8	93.9	34.1	92.9		0.01
DSC	156	66.2	97.8	34.4	92.7	158 ± 150	85
	335	68.6	96.4	34.6	93.6	111 ± 150	27
	504	70.2	96.5	35.0	94.7	135 ± 150	43

[a] $T°$ is the temperature at which the intrinsic free energy $\Delta G°$ is equal to zero and should be independent of concentration. [b] ΔC_p was estimated from the observed difference of the heat capacity of unfolded and native states. These heat capacity differences are very small and within the limit of calorimetric detection. [c] SSR is the sum of the squared residuals of the fit.

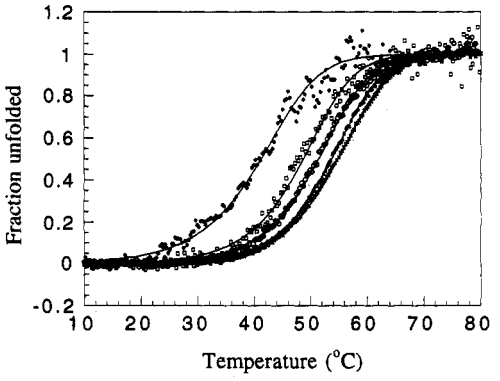

FIGURE 4: Fraction of GCN4 unfolded at different concentrations as a function of temperature. The concentrations are 1 μM (diamonds), 2 μM (squares), 5 μM (circles), 10 μM (triangles), and 20 μM (crosses). The fraction unfolded was monitored by the ellipticity at 222 nm using CD spectroscopy as described above. Experimental data are presented by symbols. Theoretical curves generated with the parameters shown in Table I are represented by solid lines.

imental data obtained by nonlinear least squares analysis. These parameters have been summarized in Table I.

A transition like the one described above, in which the population of intermediates can be assumed to be zero, can be described by simplified forms of eqs 1 and 5. In this case

$$P_U = K[(K^2 + 4)^{1/2} - K)]/2 \quad (6)$$

where

$$K = \exp(-\Delta G°/RT)/(2[P_T])^{1/2}$$

and

$$\langle \Delta H \rangle = P_U \Delta H_U(T) \quad (7)$$

The CD experiments were also analyzed in terms of the above formalism. In this case eq 6 was used to analyze the CD data normalized as described under Materials and Methods. Since the baselines were well-defined, it was not necessary to include them in the fitting procedure. The experimental data and the results of the analysis are illustrated in Figure 4. In this case GCN4 concentrations as low as 1 μM could be used, thus extending the overall concentration range studied to 1–500 μM. As shown in the figure and in Table I, similar parameter values were obtained from the analysis of the calorimetric and spectroscopic data. At $T°$ the enthalpy change measured calorimetrically averages 34.7 ± 0.3 kcal (mol of monomer)$^{-1}$ compared to the value of 35 ± 1.1 kcal (mol of monomer)$^{-1}$

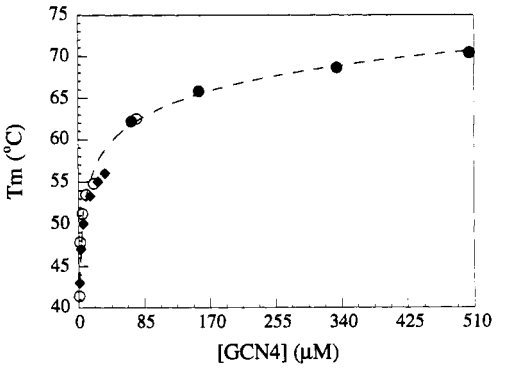

FIGURE 5: Transition temperature of GCN4 as a function of concentration. The open circles represent CD data, the filled circles represent DSC data, and the filled diamonds represent data taken from O'Shear et al. (1989). The scored line is a best fit logarithmic curve through our CD and DSC data.

measured spectroscopically, while the entropy change determined calorimetrically is 93.7 ± 0.8 cal K^{-1} (mol of monomer)$^{-1}$ at $T°$ and the one determined spectroscopically is 95.3 ± 2.9 cal K^{-1} (mol of monomer)$^{-1}$. The $T°$ value determined calorimetrically averages 96.9 ± 0.6 °C while that determined spectroscopically is equal to 94.1 ± 0.2 °C. The slight difference of 2.8 °C is most likely due to the existence of temperature gradients and/or heat losses in the spectropolarimeter, since the control and measurement of temperature in this instrument are not are precise as in the calorimeter.

The model described above and the resulting parameters accurately reproduce the concentration dependence of the transition temperature, as shown in Figures 1 and 4 and summarized in Figure 5. In this figure the transition temperatures for the two sets of data have been plotted as a function of the concentration of GCN4. The entire set of transition temperatures covers an interval of 30 °C for the concentration range studied. For comparison, the data previously published by O'Shea et al. (1989) have been included in the figure.

Structural Thermodynamic Calculations. The crystal structure of the GCN4 leucine zipper region (O'Shea et al., 1991) was used to perform structural thermodynamic calculations as described earlier for other proteins (Murphy & Freire, 1992; Murphy et al., 1992; Plaza del Pino et al., 1992). Briefly, it has been found that in the absence of, or after correction for, protonation effects the heat capacity and enthalpy changes can be written in terms of the changes in the solvent-accessible polar and apolar surface areas associated with the folding/unfolding transition. The heat capacity change can be parametrized as

$$\Delta C_p = \Delta A_{ap} \Delta C_{p,ap}° + \Delta A_{pol} \Delta C_{p,pol}° \quad (8)$$

where ΔA_{ap} and ΔA_{pol} represent the changes in accessible apolar and polar surface areas, respectively, and $\Delta C_{p,ap}°$ and $\Delta C_{p,pol}°$ the elementary ΔC_p contributions per mole of Å^2. $\Delta C_{p,ap}°$ and $\Delta C_{p,pol}°$ have been estimated as 0.45 ± 0.02 cal K^{-1} (mol·Å^2)$^{-1}$ and −0.26 ± 0.03 cal K^{-1} (mol·Å^2)$^{-1}$. At any temperature T, the enthalpy change can be written in terms of the polar and apolar contributions as

$$\Delta H(T) = \Delta H^* + \Delta C_p[T - T_H^*] \quad (9)$$

where ΔH^* is the enthalpy change at the reference temperature T_H^* = 100 °C. It has been shown that ΔH^* scales linearly with the buried polar surface area and is equal to 35 ± 1 cal (mol·Å^2)$^{-1}$ of buried polar surface that becomes exposed to the solvent. The changes in solvent-accessible surface area associated with the unfolding of the leucine zipper of GCN4

Table II: Structural Thermodynamic Analysis of GCN4

	ΔA_{pol} (mol·Å^2)	ΔA_{ap} (mol·Å^2)	$\Delta H(70)$ (kcal mol^{-1})	ΔC_p [cal (K·mol)$^{-1}$]
native dimer	1179	1470	31	354
bent helices	1015	783	33	88
standard helices[a]	1157	574	42	−43
interface (→bent)[b]	165	687	−2.2	266
interface (→standard)[c]	22	896	−11	397

[a] The structures of the standard helix conformations were generated by energy minimization using the program CHARMM (Brooks et al., 1983). [b] Represents the contribution of the interface for the process in which the native dimer separates into "bent" helices. [c] Represents the contribution of the interface for the process in which the native dimer separates into "standard" helices. All parameters are expressed on a per mole of monomer basis.

are summarized in Table II. Equations 8 and 9 predict a $\Delta C_{p,U}$ of 350 cal (K·mol)$^{-1}$ and a $\Delta H_U(70)$ of 31 kcal mol^{-1}. The experimental values are 135 ± 150 cal (K·mol)$^{-1}$ and 31.5 kcal mol^{-1}, respectively. The theoretical and experimental values are very close in magnitude, further supporting the notion that the heat effect observed during thermal unfolding arises from the unfolding of the leucine zipper itself and that the basic region of GCN4–56 does not contribute to the stability. Presumably this region is unstructured throughout the entire temperature range considered, as also indicated by the CD data.

The structural thermodynamic approach outlined above allows a dissection of the contributions arising from the folding of the individual helices and the formation of the interface between the two strands in the coiled coil. For the purpose of dissecting the energetic contributions, we consider the following states: (1) the intact dimer (N_2); (2) the individual helices preserving the structure that they assume in the coiled coil ("bent helices" are abbreviated B); (3) the isolated helices in a standard helical conformation ("standard helices" are abbreviated S); and (4) the unfolded state (U). The energetic contribution associated with the transformation of the interface (int) to the bent and standard helices is also explicitly considered in this analysis. Table II summarizes the polar and apolar surface areas buried from the solvent by each of these conformations. As shown below, the sum of these contributions accounts for the overall enthalpy (−31.5 kcal mol^{-1}) and the entropy [−84.7 cal (K·mol)$^{-1}$] of formation of the dimer at the experimental transition temperature (70 °C).

According to the data in Table II, the formation of the standard helices involves the burial of 1157 and 574 Å^2 of polar and apolar surface, respectively. These values are consistent with a small, slightly positive ΔC_p for helix formation, in agreement with previous results for other α-helices (Freire & Murphy, 1991). The enthalpy difference between the standard helix and the unfolded state ($\Delta H_{U\rightarrow S}$) is −42 kcal mol^{-1} at 70 °C. This number is consistent with a ΔH of −1.4 kcal mol^{-1} for the formation of one hydrogen bond, in agreement with the direct calorimetric measurements of Scholtz et al. (1991). As summarized in Table II, the bending of the α-helix buries 209 Å^2 of apolar surface area, and the formation of the dimer interface results in the burial of an additional 687 Å^2 for a total of 896 Å^2. By comparison, the bending of the helices and formation of the dimer interface involve essentially no additional change in the magnitude of the buried polar surface. The overall process of bending the helices and forming the dimer interface contributes a $\Delta C_{p,S\rightarrow N_2}$ of −397 cal (K·mol) and a $\Delta H_{S\rightarrow N_2}$ of 11 kcal mol^{-1} at the experimental transition temperature of 70 °C.

The above results are consistent with the structural observation that the interface between the two helices is predominantly hydrophobic. Accordingly, most of the positive ΔC_p observed upon unfolding arises from the exposure to the solvent of the hydrophobic surface at the interface between the helices. Conversely, most of the positive enthalpy of unfolding at the transition temperature arises from the unfolding of the helices themselves. The disruption and exposure of the interface to water is accompanied by a small negative enthalpy.

It must be noted that the enthalpy change for the folding/unfolding transition of a standard helix is only slightly temperature dependent. Since ΔC_p for unfolding of the standard helix is −42 cal K^{-1} (mol of monomer)$^{-1}$, the enthalpy change for the unfolding of the standard helices of GCN4 is expected to vary only 4 kcal (mol of monomer)$^{-1}$ between 0 and 100 °C. Although the formation of individual α-helices is enthalpically favorable at all temperatures, the experimental evidence presented in this paper clearly indicates that the isolated helices of GCN4 are not intrinsically stable under the conditions studied since they never become significantly populated. As shown below, the favorable enthalpy of forming the individual helices in GCN4 in insufficient to overcome the unfavorable entropy associated with ordering the peptide chain in this helical conformation.

Since the formation of the interface is enthalpically unfavorable ($\Delta H_{S\rightarrow N_2}$ = 11 kcal mol^{-1}), it is apparent that the remaining favorable contributions to the free energy of stabilization of the dimer must come from a positive entropy change associated with the formation of the coiled coil. The main source of favorable entropy is solvent related and is due to the burial of apolar surface, as reflected by the large negative ΔC_p associated with the formation of the interface (hydrophobic effect). The burial of predominantly hydrophobic residues upon formation of the interface is expected to contribute a positive entropy close to 46 cal (K·mol^{-1}) at the experimental transition temperature of 70 °C. To stabilize the leucine zipper, this favorable entropy must overcome the unfavorable configurational entropy of structuring the peptide chain as well as the entropy of associating the two strands. The configurational entropy change associated with structuring the entire dimer is on the order of −130 cal K^{-1} (mol of monomer)$^{-1}$ [see Murphy and Freire (1992) and Murphy et al. (1993)]. Furthermore, the cratic entropy term arising from the loss of translational entropy due to the association process itself is close to −4 cal K^{-1} (mol of monomer)$^{-1}$ (Kauzmann, 1959). The sum total of the entropy contributions mentioned above is −88 cal (K·mol)$^{-1}$, which is already very close to the experimental entropy change of −84.7 cal (K·mol)$^{-1}$ at 70 °C. These values suggest that an additional entropic contribution of approximately 3 cal (K·mol) (i.e., ~1− kcal mol^{-1} to the Gibbs free energy of stabilization) is necessary to account for the experimentally observed transition temperature.

The interactions listed above provide the bulk of the favorable Gibbs free energy required for stabilization. The total magnitude of the interactions, however, appears not to be sufficient to completely account for the observed transition temperature of 70 °C; consequently, another source of favorable Gibbs free energy might be required. This is most likely provided by electrostatic interactions (also primarily entropic) as described by O'Shea et al. (1991) and not included in the above analysis. These authors observed electrostatic complementary provided by alternating positive and negative residues along the helices and suggested the formation of

interhelical ion pairs between Lys^{15} and $Glu^{20'}$, Glu^{22} and $Lys^{27'}$, and $Glu^{22'}$ and Lys^{27}. In addition, two intrahelical ion-pair interactions are observed for a total of five within the intact dimer. The contribution of ion pairs to the free energy of stabilization is not accurately known; however, for ion pairs fairly exposed to the solvent as in GCN4, it is estimated to be on the order of 1 kcal mol^{-1} (Fersht, 1973; Perutz & Raidt, 1975). If this is the case, electrostatic interactions can be expected to modulate the exact value of the transition temperature by as much as 20 deg.

For proper optimization of the free energy of stabilization, a precise structural matching of the hydrophobic surfaces and the location of ion pairs is required. Since the strength of the hydrophobic interaction is proportional to the apolar surface area that becomes buried from the solvent, a tight packing of the hydrophobic residues provides a better stabilization of the zipper. Along these lines, O'Shea et al. (1991) noted that compared to linear aliphatic side chains, branched ones (such as leucine) pack better with neighboring residues and make closer contacts with the adjacent layers in the interface. Similarly, electrostatic interactions are maximized by alternating the location of positive and negative residues along the zipper.

CONCLUSIONS

It has been demonstrated that the folding/unfolding transition of GCN4 is highly cooperative and is characterized by the absence of folded monomers. Under the experimental conditions, native dimers and unfolded monomers account for essentially the entire population of molecules. Further, it has been shown that the thermodynamic stability of a leucine zipper results from a delicate combination of hydrophobic and electrostatic interactions, as originally suggested by O'Shea et al. (1991). Since the helices are intrinsically unstable within the temperature range studied, the interactions at the interface must provide the necessary additional free energy of stabilization. The bulk of the interaction at the interface is hydrophobic ($\sim$4 kcal mol^{-1}), but electrostatic interactions ($\sim$1 kcal mol^{-1}) appear to play a significant modulatory role. This conclusion is structurally and functionally important since these two effects require a tight complementary between the two helices in the zipper. These results agree with the observed stability and dimerization differences between various leucine zippers (O'Neil et al., 1991) and the structural observation that a heptad repeat of leucines is, by itself, no sufficient to mediate dimerization (O'Shea et al., 1991). The observed differences in stability appear to be significantly influenced by electrostatic interactions.

ACKNOWLEDGMENT

We thank Professor Jon D. Shuman for generously providing GCN4–56 peptide and Professor Tom Alber for providing the coordinates to the crystal structure.

REFERENCES

Agre, P., Johnson, P. F., & McKnight, S. L. (1989) *Science 246*, 922–926.
Brooks, R. R., Bruccoleri, R. E.; Olafson, B. D., States, D. J., Swaminanthan, S., & Karplus, M. J. (1983) *J. Comput. Chem. 4*, 187–217.
Crick, F. H. C. (1953) *Acta Crystallogr. 6*, 689–697.
Fersht, A. R. (1972) *J. Mol. Biol. 64*, 497–509.
Freire, E. (1989) *Comments Mol. Cell. Biophys. 6*, 123–140.
Freire, E., & Biltonen, R. L. (1978) *Biopolymers 17*, 463–479.
Freire, E., & Murphy, K. P. (1991) *J. Mol. Biol. 222*, 687–698.
Gentz, R., Rauscher, F. J., Abate, C., & Curran, T. (1989) *Science 243*, 1695–1699.
Johnson, P. F., & McKnight, S. L. (1989) *Annu. Rev. Biochem. 58*, 799–839.
Kauzmann, W. (1959) *Adv. Protein Chem. 14*, 1–63.
Landshultz, W. H., Johnson, P. F., & McKnight, S. L. (1988) *Science 240*, 1759–1764.
Landshultz, W. H., Johnson, & McKnight, S. L. (1989) *Science 243*, 1681–1688.
Lee, B., & Richards, F. M. (1971) *J. Mol. Biol. 55*, 379–400.
Murphy, K. P., & Freire, E. (1992) *Adv. Protein Chem. 43*, 313–361.
Murphy, K. P., Bhakuni, V., Xie, D., & Freire, E. (1992) *J. Mol. Biol. 227*, 293–306.
Murphy, K. P., Xie, D., Garcia, K. C., Amzel, L. M., & Freire, E. (1993) *Proteins 15*, 113–120.
Oas, T. G., McIntosh, L. P., O'Shea, E. K., Dahlquist, F. W., & Kim, P. S. (1990) *Biochemistry 29*, 2891–2894.
O'Neil, K. T., Hoess, R. H., & DeGrado, W. F. (1990) *Science 249*, 774–778.
O'Neil, K. T., Shuman, J. D., Ampe, C., & Degrado, W. F. (1991) *Biochemistry 30*, 9030–9034.
O'Shea, E. K., Rutkowski, R., & Kim, P. S. (1989) *Science 243*, 538–542.
O'Shea, E. K., Klemm, J. D., Kim, P. S., & Alber, T. (1991) *Science 254*, 539–544.
Perutz, M. F., & Raidt, H. (1975) *Nature 255*, 256–260.
Plaza del Pino, I. M., Pace, C. N., & Freire, E. (1992) *Biochemistry 31*, 11196–11202.
Privalov, P. L., & Gill, S. J. (1988) *Adv. Protein Chem. 39*, 191–234.
Ramsay, G., & Freire, E. (1990) *Biochemistry 29*, 8677–8683.
Rasmussen, R., Benbegnu, D., O'Shea, E. K., Kim, P. S., & Alber, T. (1991) *Proc. Natl. Acad. Sci. U.S.A. 88*, 561–564.
Saudek, V., Pasley, H. S., Gibson, T., Gausepohl, H., Frank, R., & Pasore, A. (1991) *Biochemistry 30*, 1310–1317.
Scholtz, J. M., Marqusee, S., Baldwin, R. L., York, E. J., Stewart, J. M., Santoro, M., & Bolen, D. W. (1991) *Proc. Natl. Acad. Sci. U.S.A. 88*, 2854–2858.
Shuman, J. D., Vinson, C. R., & McKnight, S. L. (1990) *Science 249*, 771–774.
Turner, R., & Tjian, R. (1989) *Science 246*, 1689–1694.
Vinson, C. R., Sigler, P. B., & McKnight, S. L. (1989) *Science 246*, 911–916.
Weiss, M. A. (1990) *Biochemistry 29*, 8020–8024.
Weiss, M. A., Ellenberger, T., Wobbe, C. R., Lee, J. P., Harrison, S. C., & Struhl, K. (1990) *Nature 347*, 575–578.
Xie, D., Bhakuni, V., & Freire, E. (1991) *Biochemistry 30*, 10673–10678.